

Article

Topological Optimization of Interconnection of Multilayer Composite Structures

P. V. Dunchenkin ¹, V. A. Cherekaeva ¹, T. V. Yakovleva ^{1,*} and A. V. Krysko ^{2,*} 

¹ Department of Mathematics and Modeling, Yuri Gagarin State Technical University of Saratov, 77 Politehnicheskaya Str., 410054 Saratov, Russia

² Department of Applied Mathematics and Systems Analysis, Yuri Gagarin State Technical University of Saratov, 77 Politehnicheskaya Str., 410054 Saratov, Russia

* Correspondence: yan-tan1987@mail.ru (T.V.Y.); anton.krysko@gmail.com (A.V.K.)

Abstract: This study focuses on the topological optimization of adhesive overlap joints for structures subjected to longitudinal mechanical loads. The aim is to reduce peak stresses at the joint interface of the elements. Peak stresses in such joints can lead to failure of both the joint and the structure itself. A new approach based on Rational Approximation of Material Properties (RAMP) and the Finite Element Method (FEM) has been proposed to minimize peak stresses in multi-layer composite joints. Using this approach, the Mises peak stresses of the optimal structural joint have been significantly reduced by up to 50% under mechanical loading in the longitudinal direction. The paper includes numerical examples of different types of structural element connections.

Keywords: topological optimization; RAMP; adhesive joints; finite element method; mises stresses; shear stresses



Citation: Dunchenkin, P.V.; Cherekaeva, V.A.; Yakovleva, T.V.; Krysko, A.V. Topological Optimization of Interconnection of Multilayer Composite Structures. *Computation* **2023**, *11*, 87. <https://doi.org/10.3390/computation11050087>

Academic Editors: Martynas Patašius and Rimantas Barauskas

Received: 14 March 2023

Revised: 18 April 2023

Accepted: 22 April 2023

Published: 25 April 2023



Copyright: © 2023 by the authors. Licensee MDPI, Basel, Switzerland. This article is an open access article distributed under the terms and conditions of the Creative Commons Attribution (CC BY) license (<https://creativecommons.org/licenses/by/4.0/>).

1. Introduction

In various industrial and technological applications, joining elements of composite structures using a third phase is common due to its ease and durability [1–4]. These methods include traditional adhesive bonding, soldering, brazing, welding, riveting, and others. Recent developments in vehicle design, particularly in automobiles and aircraft, aim to create products with low weight and high durability, leading to increased interest in adhesive bonding. However, under longitudinal and transverse loads, the joints experience peak stresses that can cause them to fail. To overcome this problem, overlap joints are commonly used due to their manufacturability, and the reliability of such joints can be increased by changing the thickness of the adhesive, its composition, the type of joint, or the shape of the outer surface of the adhesive layer at the edges of the joint.

One of the most important geometric factors is the thickness of the adhesive layer between the joints, as it significantly affects the stress-strain state of the joints. Kahraman et al. [5] report on a study of the effects of adhesive thickness and aluminum filler content on the mechanical performance of aluminum joints bonded with epoxy resin and aluminum powder. The authors investigated, both experimentally and numerically using FEM, the influence of adhesive thickness and aluminum filler content on the bond strength of the joints. They showed that, in general, the bond strength decreases with increasing adhesive thickness. The joints failed in the cohesive mode (adhesive failed) due to the high stress level generated by the adhesive. This indicates that the adhesion to the metal surface is stronger than the adhesion to the inside of the adhesive. Grant et al. [6] described lap joints of two steel parts joined by epoxy and investigated the problems of structural tension (which creates shear along the joint line), pure bending, and bending plus shear. They considered the influence of various parameters on the strength of the joint, including the length of the overlap, the thickness of the bonding line, and the change in the shape of the outer surface of the adhesive layer at the edges of the joint. M.N. Vinay [7] carried

out experimental studies on the effect of adhesive layer thickness, overlap length, and surface roughness on the strength of a double symmetric overlap joint. It was shown that the thickness of the adhesive layer was the most important parameter and that the strength of the bond decreased when the thickness was reduced or increased beyond the optimum level.

The stiffness of adhesive joints has been studied for static loads, dynamic loads, and impact. Yaman et al. [8] studied the effect of adhesive thickness, overlap length, number of layers, and orientation of adhesive fibers on the natural frequency and damping of two- and three-part adhesive joints. They compared the FEM results with the experimental analysis data. The studies showed that the thickness and orientation angle of the adhesive fibers were the main parameters that changed the position of the resonant frequency of the structure. In the study by Kemiklioglu et al. [9], the authors investigated the effect of different vibration loads on the failure mechanisms of adhesive composites. The study found that the strength of adhesive joints under vibration was lower than that of non-vibration joints. Yaman et al. [10] conducted an experimental study to investigate the natural frequencies and damping coefficients of adhesive single strap joints (SSJ) and double strap joints (DSJ). The results indicated that DSJ had better damping properties than single-lap joints (SLJ) and SSJ. Moreover, the thickness of the adhesive had a more pronounced effect on the damping properties than the overlap length. Almitani et al. [11] proposed a solution for determining the effect of dynamic loading on the adhesive bond using an improved dissipation model. They compared the analytical solution obtained in the paper with the results of the finite element method. It was concluded that the eigen-frequencies are mainly influenced by the damping coefficient of the substrates rather than the damping coefficient of the adhesive joint. Machado et al. [12] investigated the strength and fracture resistance of single-layer overlap joints under impact loading. The study was carried out on two types of adhesive with high stiffness and high ductility. They investigated the effect of the cohesive parameters of the adhesive by varying each of these parameters while maintaining the others.

Dragoni et al. [13] derived analytical formulae for the relative stiffness of the beam—adhesive—beam, which were used to find the optimum joint parameters. The finite element method was used to verify the relationships obtained for three types of connections between two beams. The analytical formulae for optimization by fitting determine the dimensions of the multilayer beam that maximize either the stress uniformity along the bond line or the test sensitivity to the shear modulus of the adhesive. It was shown that the two conditions cannot be achieved simultaneously.

It should be noted that no optimization procedures were used in all the work, and the joint strength improvement was completed with a simple overshoot. However, numerical optimization techniques, particularly topological optimization, are not used.

Fedorov et al. [14] proposed a method for selecting the mechanical characteristics and geometric parameters of an interlayer bond of two similar or different materials to avoid significant stress concentrations near the edges of both interfaces. They solved a number of model examples to optimize the characteristics and geometry of the adhesive layer to minimize stress concentration at the interface. The proposed approach is more intuitive and allows a mathematical theory to be constructed. Valente et al. [15] determined the maximum load values at which a lap joint breaks on impact using cohesive zone models. They performed modifications of the lap joint geometry by introducing external and internal chamfers in the adhesives, as well as adding adhesive ridges, to observe the effects of these modifications with different types of adhesives. In this way, the optimum type of adhesive joint was obtained by simple overshooting, which is not optimal from a design point of view. The study by the same authors [16], with a similar approach to joint optimization, is devoted to a numerical study of the cohesive zone of tensile-loaded lap joints in impact scenarios with three adhesives with different properties.

The analysis of the above studies shows that the problem of smoothing the peak stresses at the joints of structural elements has not been solved yet. Available experimental

studies have shown that the failure of structures occurs at the joints. This problem can be solved using numerical optimization algorithms, in particular topological optimization.

Ejaza et al. [17] used a nonparametric optimization algorithm to optimize the structure of three types of overlap girder joints to reduce peak stresses in the adhesive layer. Topological optimization of the selected adhesive joints was carried out to determine the optimum topology and shape of the adhesives and side bevels. To solve the optimization problems, the approach of minimizing the yield strength was used, which, in terms of energy, is equivalent to minimizing the total energy of deformation. A standard topological optimization procedure in the Abaqus module was used. The gain from the optimization was up to 38% for shear stress. Vicente et al. [18,19] used topological optimization of the adhesive used as a joint for the elements used in the construction of ship hulls. In ref. [18], the behavior of overlap joints of metal-hybrid panels with primary structural elements in a ship's structure was investigated. Topological optimization was applied to minimize the Mises solder stress. In ref. [19], the joint geometry is optimized by topological optimization of a symmetrical steel part in the form of a clamp, attaching a hybrid panel using structural adhesive. The objective function of the optimization problem to be solved is defined as the total mass of the steel part, which should be as light as possible. The geometric shape resulting from this optimization is analyzed using finite elements by simulating a non-linear cohesive zone model, minimizing von Mises stresses. The weight of the structure, after applying the optimization procedure, is 16.4% less than that of the original design. Kim et al. [20] propose a method to prevent the separation of adhesive bonds between different material phases while optimizing the topology. The interfacial tension energy density (ITED) is introduced into the target function to limit the formation of areas where the material interface with the adhesive is subjected to tensile stress. Optimization examples for different types of beams loaded with concentrated forces at the free end are considered. Results for topological optimization with and without ITED consideration are compared. Consideration of ITED gives a greater load carrying capacity of the beam.

Note that the paper does not provide a comparison with results obtained by other authors.

Arhore et al. [21] investigated the effect of external adhesive geometry on the strength of an adhesively bonded joint using two different numerical optimization methods: genetic algorithm (GA) and topology optimization (TOP). The joint consisted of composite inner and outer fasteners. The results also showed that the strength of the connection subjected to bending loads is independent of the external connection geometry, thus minimizing its weight. A comparison of different approaches to joint optimization in terms of solution time and quality is presented. The Mallick monograph [22] provides background information on various aspects of optimal design and performance improvement of adhesive joints in building structures. These include joint configurations, joint design parameters, substrate properties, and adhesive selection. Methods to improve joint performance by modifying the adhesive layer, shaping the substrate, and hybrid jointing are presented. Hamdia et al. [23] optimized a flexoelectric composite composed of flexoelectric and purely elastic building blocks. The direct problem was solved using isogeometric analysis (IGA) with a Non-Uniform Rational B-Spline (NURBS). The optimization problem was solved using a multilevel Monte Carlo (MLMC) method based on genetic algorithms (GA). The results showed that the proposed method reduced computational costs in numerical experiments without any loss of accuracy. Krysko et al. [24,25] have proposed an approach based on methods for topological optimization of adhesive joints in order to minimize stresses in the adhesive layer and the structure itself. The study [24] proposed and substantiated an approach to obtaining an optimal structure and distribution of gradient material properties to reduce stress levels in a brazed joint. The approach is based on a combination of topological optimization methods (moving asymptote method) and finite element methods. Several examples have been considered that confirm the performance of the proposed approach. Study [25] is devoted to the problem of the strength of two overlapping elements glued together under mechanical loads, based on Solid Isotropic Material with Penalty (SIMP) and finite element methods, where the design variable is the material density of the

structure. The results were compared with those obtained using engineering calculations and were optimized by 20%.

In engineering practice, an experimental approach is often used for calculating joints in multilayer composite structures. This approach involves selecting different connection options and adhesives with the best physical and chemical properties, which has yielded positive results. However, there is still an issue with optimizing these joints to reduce peak Mises and shear stresses. A review of the scientific literature reveals that there are publications based on genetic algorithms [17–21] addressing this issue.

It should be noted that it is practically possible to create an optimum design of welded joints obtained by topological optimization by means of a 3D printer. There are several studies in the scientific literature on the use of topological optimization to create optimal structures’ designs, which can be printed on a 3D printer. For instance, [26] presents a topological optimization-based design structure for multifunctional 3D printing and notes that the Center for Innovative Additive Manufacturing at the University of Nottingham and Loughborough, UK, has as one of its primary goals to develop multifunctional 3D printing processes. In addition to this article, references can be made to [27,28].

There is a lack of scientific literature on the optimization of adhesive bonds that are subject to structural failure. However, notable works include those of Krysko et al. [24,25], who developed an approach to reduce peak stresses at joints using a combination of finite element and moving asymptote methods. In this paper, we present a further development of this approach, using the RAMP method and FEM to join multilayer composites. This new approach resulted in a reduction in peak Mises stresses of up to 50%. On the other hand, the classical engineering approach did not result in any reduction of the peak stresses in the Mises joint.

The paper is structured as follows: Section 2 describes the formulation of the topological optimization problem, including the forward problem and the inverse solder optimization problem. Section 3 presents and discusses the numerical results of the implementation. Finally, Section 4 of the paper discusses some results and concludes the study.

2. Peak Stress Minimization Based on RAMP and FEM Techniques for Multilayer Composite Joints

2.1. Statement of the Direct Problem

Consider an area Ω consisting of three sub-areas $\Omega_i, i = 1, 2, 3$ (Figure 1), which are interconnected. One of the sub-areas Ω_3 is the solder layer. We denote $E_i(\mathbf{x}), \mathbf{x} = \{x_1, x_2\}, i = 1, 2, 3$ the Young’s modulus of elasticity in the subdomains Ω_i , respectively. The two-dimensional elastic region Ω is bounded by a closed surface $\Gamma = \Gamma_1 \cup \Gamma_2 \cup \Gamma_3$, and it is assumed that the material is isotropic and linearly elastic.

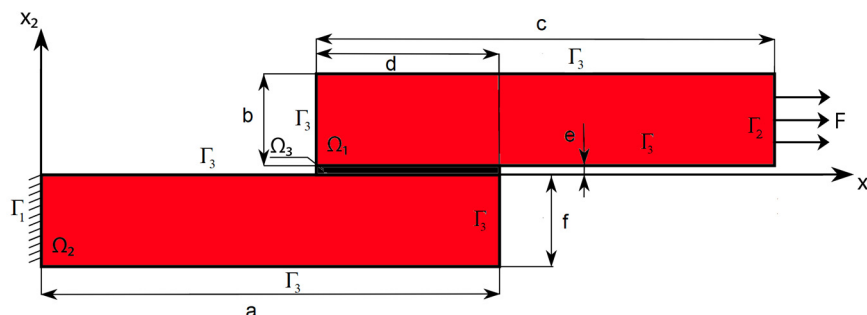


Figure 1. Design and boundary conditions.

Boundary conditions: At the boundary $\Gamma_1 \in \Omega_2$ —a fixed support boundary condition $\{u_i(\mathbf{x}) = 0, i = 1, 2\}$ is defined. At the boundary $\Gamma_2 \in \Omega_1$ a load of intensity F is applied. The boundary Γ_3 is free from loads.

The relationship between deformations and displacements is determined by:

$$\varepsilon_{ij} = \frac{1}{2}(u_{i,j} + u_{j,i}), \quad i, j = 1, 2 \quad (1)$$

The stress-strain relation for a plane stress state is written as follows

$$\sigma_{11} = E(\mathbf{x})\varepsilon_{11}, \quad \sigma_{12} = 2G(\mathbf{x})\varepsilon_{12} \quad (2)$$

The equilibrium equation is as follows:

$$\sigma_{ij,j} = 0, \quad (i, j = 1, 2) \text{ in } \Omega, \quad (3)$$

where σ_{ij} is the stress tensor.

2.2. Statement of the Topological Optimization Problem

Experimental analysis of brazed joints has shown that the highest shear stresses occur in the solder due to its small thickness. The maximum shear stresses are present at the ends of the solder layer and are minimal in the middle of the solder layer. Therefore, the goal of the optimization problem of topological optimization of the interconnection of multilayer composite structures is to reduce the peak shear stresses in the solder layer. Among the algorithms used for topological optimization, such as homogenization [29], SIMP [30], ESO [31], and the RAMP approach [32], SIMP and RAMP methods are the most popular. While the SIMP method implies high efficiency in a narrow range of problems, the RAMP method is a stable method that can be used in a wider class of problems [33]. Therefore, the authors of this paper used the RAMP method. The choice of the RAMP method is also determined by the fact that the RAMP interpolation scheme is able to ease the issues associated with the formation of “gray material” compared with the SIMP scheme. “Gray material” appears in many topological optimization results when using density-based methods as a region of intermediate gray material. In practical applications, these areas cannot be physically realized. It is necessary to achieve a clearer phase separation of the materials used. In contrast to SIMP, RAMP interpolation has a sensitivity other than zero at a density of zero. RAMP is used in combination with the finite element method to solve the direct problem of elasticity theory, but with one modification: For each finite element in the partitioning area, only one design variable is defined, denoting the material density of the current element.

The power-law interpolation function for regions containing voids and one phase of the material has the form:

$$E_e(\rho_e) = \rho_e^p E_e^0, \quad 0 < \rho_{\min} \leq \rho_e \leq 1, \quad (4)$$

where E_e is the modulus of elasticity of the material in the finite element, E_e^0 —modulus of elasticity of the base (originally specified) material, $p \geq 1$ —a penalty parameter, and increasing it leads to a better solution to the optimization problem. The p -value was chosen to be either 4 or 5, according to the recommendations given in Bendsøe [34]. The design variable ρ_e is bounded from below by a constant ρ_{\min} , introduced to prevent degeneracy of the finite element matrix.

Note that for the values of $\rho_{\min} \leq \rho_e \leq 1$, the modulus $E_e(\rho_e)$ is limited to the lower threshold of the density $\rho_e = \rho_{\min}$ and the value of Young’s modulus of the phase of the base material E_e^0 , for $\rho_e = 1$.

In the topological optimization phase, the structure with the highest stiffness must be obtained by changing the geometry of the “optimization areas” and the amount of material bonded by the adhesive layer accordingly, without changing the original material. A change in the amount of material in a finite element (or group of elements) should result in a reduction of stresses both in the optimization areas and in the adhesive area, which is

most susceptible to fracture. In order to obtain the design with the highest stiffness, the RAMP method minimizes the strain energy W_s by increasing the density in the areas with more pronounced sensitivity. The strain energy determines the target function:

$$f_t = \frac{1}{W_{s0}} \int_{\Omega} W_s(x) d\Omega \tag{5}$$

where Ω —area of the structure considered (merging areas Ω_1 and Ω_2), W_{s0} —normalizing factor.

At the same time, restrictions on the amount of material for the modelling must be met in the area where the optimization problem is solved

$$0 \leq \int_{\Omega} \rho(\mathbf{x}) d\Omega_{opt} \leq \gamma A, \tag{6}$$

where: A —optimized area Ω_{opt} , γ —material volumetric ratio.

Experimental analysis of brazed joints has shown that the highest shear stresses occur in the solder due to its small thickness. The maximum shear stresses are present at the ends of the solder layer and are minimal in the middle of the solder layer. Therefore, the goal of the optimization problem is to reduce the peak shear stresses in the solder layer.

The numerical interpretation of the topological optimization problem leads to two issues: the “checkerboard” problem and the problem of dependence of the optimal solution on the grid. Mesh dependency, which arises from the fact that a finer mesh allows for sharper optimal designs, can be mitigated by increasing the number of partitions. The authors of this work addressed this issue in their studies on the optimization of structures [24,25,35,36] as well as the identification of holes/inclusions [37,38].

The “checkerboard” problem refers to the formation of adjacent elements with high and low density, arranged in a checkerboard pattern. To mitigate the checkerboard effect in the optimal structure, a penalty function is typically introduced in the form

$$f_p = \frac{h_0 h_{max}}{A} \int_{\Omega} |\nabla \rho(\mathbf{x})|^2 d\Omega, \tag{7}$$

where: h_0 —initial grid size, which controls the size of the elements in the split, h_{max} —the current size of the element at the given level. The penalty function is dimensionless and typically has a value of the order of unity for the worst possible solution. Dimensionless target function f_t (5) and penalty function f_p (7) must be consistent, for example, in the form of a linear combination (5) and (7) with a given parameter q , i.e., we have

$$f = \frac{1-q}{W_{s0}} \int_{\Omega} W_s(x) d\Omega + q \int_{\Omega} |\nabla \rho(x)|^2 d\Omega. \tag{8}$$

Value $0 \leq q \leq 1$ allows balance the goal function and the penalty function with each other.

Below, the effectiveness of the proposed new algorithm for the numerical implementation of minimizing peak stresses in multilayer composite structures using the finite element method (FEM) is demonstrated through simulations conducted with the Comsol Multiphysics package.

3. Numerical Results

3.1. Case Study 1. Optimization of the Lap Joint of a Two-Layer Package

Consider a scarf joint, a technique where two areas are joined, overlapping at an angle, and glued together. In our case, let’s study a two-layer isotropic package (Ω_1, Ω_2) with an adhesive layer Ω_3 , the dimensions and boundary conditions of which are shown in Figure 2. Dimensions are given in mm. Area Ω_1 filled with duralumin with a Young modulus equal

to $E_1 = 73.1 \times 10^6$ Pa, Ω_2 —the solution area of the topological optimization problem involves finding the optimum microstructure for the distribution of a given amount of duralumin also with a Young modulus equal to $E_1 = 73.1 \times 10^9$ Pa and Ω_3 —area of evenly distributed adhesive solder with $E_2 = 2.26 \times 10^9$ Pa. Mechanical load acting on the right $F = 100,000 \frac{H}{m^2}$, the left border is fixed.

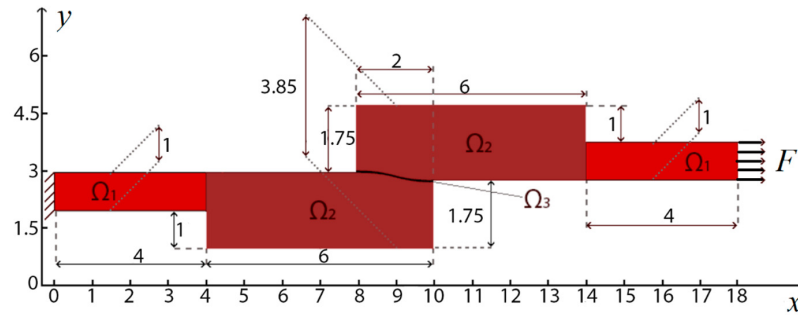
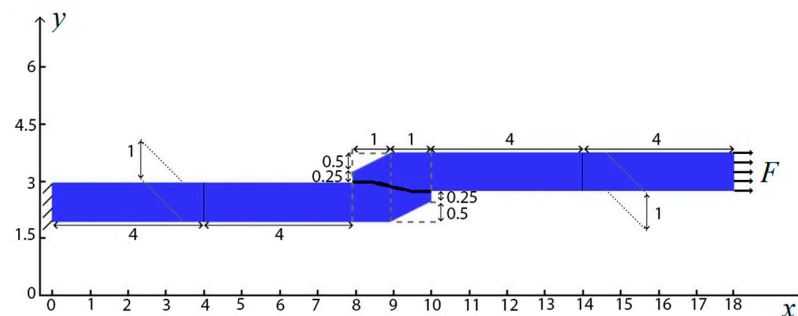
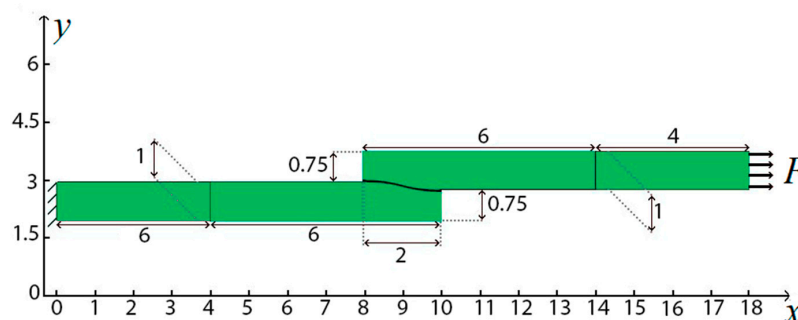


Figure 2. Case study 1. Design and boundary conditions, optimization (A). ■ Ω_1 —nonoptimized area, ■ Ω_2 —optimized area, ■ Ω_3 —adhesive.

In overlap bonding, there are discontinuities at the ends of the bond line [1–4]. These inhomogeneities lead to bending moments due to eccentric loading and uneven moment distribution around the adhesive layer, which can cause destructive stresses in the adhesive layer. Breaking the connection geometry can also produce high shear stresses in the adhesive. However, there are ways to reduce this eccentric loading in lap joints. For example, it has been shown [17] that narrowing the edges of the bonded layers is effective in reducing these stresses (Figure 3a). In addition, increasing the length of the joint, the thickness of the solder, and the thickness of the layers being joined can reduce the maximum shear and peel stresses. In our case, all geometric and physical parameters of the braze remain constant, and the reduction in maximum stresses at the ends of the braze is achieved by topological optimization of the microstructure of the layers to be joined.



(a)



(b)

Figure 3. Three-layer constructions with an adhesive layer: (a) ■ Classic type of connection with bevel (B); (b) ■ Classical connection without bevel (C).

Figure 3 illustrates the three-layer structures commonly found in practical applications (Figure 3a,b). The structure shown in Figure 3a is characterized by the beveled corners of the elements being joined, which is a classic engineering technique for reducing shear stresses. It is worth noting that the amount of duralumin and silver solder material in the structures shown in Figure 3a,b and the design in Figure 2 is the same, with the coefficient γ set to 0.5 when solving the optimization problem.

The results of topological optimization are shown in Figures 4 and 5, which display the distributions of shear stress σ_{12} and Mises stress σ_{Mis} , respectively, in the adhesive layer for the A, B, and C design cases. It should be noted that all plots for σ_{Mis} and σ_{12} hereafter are given for the line passing through the center of the adhesive layer.

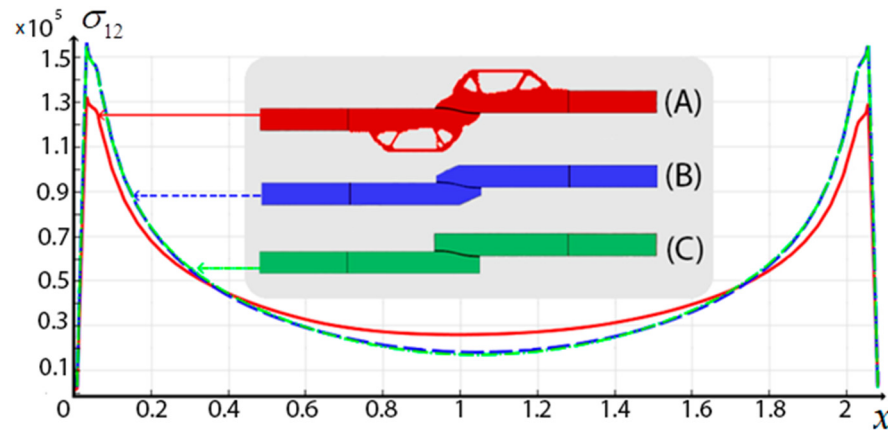


Figure 4. Shear stress (Pa) along the central axis of the solder region. (A) ■ optimal design, (B) ■ Classic type of connection with bevel, (C) ■ Classic type of connection without bevel.

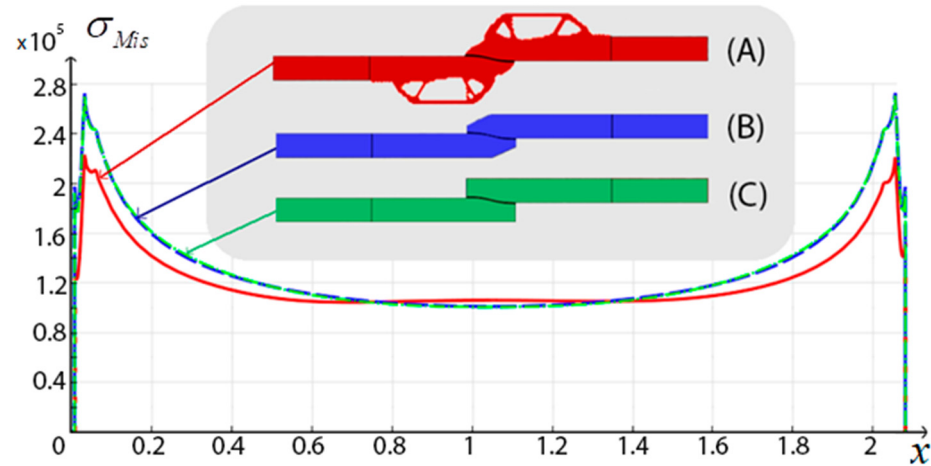


Figure 5. Von Mises stress (Pa) along the central axis of the solder region. (A) ■ optimal design, (B) ■ Classic type of connection with bevel, (C) ■ Classic type of connection without bevel.

The results of the optimization of the two-layer composite package showed that the peak Mises stresses at the edges of the adhesive were significantly reduced for the optimal design (A) compared with the stresses for (B) and (C), as shown in Figures 4 and 5. Since peak shear stresses at the edges of the adhesive can cause joint failure and ultimately lead to failure of the entire structure, stress reduction at these locations is a critical engineering application of the approach proposed by the authors.

Table 1 shows the maximum Mises stresses in the solder layer and the maximum shear stresses in the solder layer for the three Designs (A)–(C).

Table 1. Values of maximum stress for Case Study 1.

Construction	Maximum Value σ_{Mis} in Solder	Maximum Shear Stresses σ_{12} in Solder
Topologically optimal construction (A)	225,356	121,540
Bevel (engineering option to reduce the shear stress) (B)	279,400	144,320
Straight (initial design) (C)	279,250	143,941

Table 1 demonstrates that for the engineered version of shear stress reduction (B), the values of σ_{Mis} and σ_{12} are greater than those of the original design. For the topologically optimal design, the maximum values σ_{Mis} are reduced by almost 20%. Therefore, we can conclude that the proposed stress minimization algorithm is versatile for different types of solder.

As the optimization problem is based on the numerical finite element method, the reliability of the results is an important consideration. The convergence of the optimization results, depending on the number of finite elements, is investigated in Table 2 and Figure 6 using Runge’s principle with a doubling of the number of finite elements. To obtain reliable results, it is necessary to use 3.94×10^3 finite elements, as the difference from the results at 6.96×10^3 is 0.06%. This conclusion is confirmed by the points on curves I and III, where the solution stabilizes. For the middle of the joint (point II), convergence is observed at 6×10^3 finite elements. The number of iterations needed to reach a solution is practically the same. With an increasing number of finite elements, the quality of optimization improves considerably, as evidenced by the “smoothing” of shear stress values at the joint points. With a small number of partitions, the stress in the middle of the joint (point II) differs from the stress at the extreme points by almost seven times in the optimal design. However, increasing the number of finite element partitions leads to the equalization of stresses in the optimum design, with a difference of less than 39.2%.

Table 2. Dependence $\max\sigma_{12}$ from number of iterations n and σ_{12}^k from number N for FE. ■ optimal design, ■ Classic type of connection with bevel, ■ Classic type of connection within bevel.

Visualisation of the FE Approximation of an Overlapping Joint between Two Beams		Number of El-ements $N \times 10^3$	Maximum Stress $\max\sigma_{12} \times 10^5$	Number of Iterations n	I $\sigma_{12}^I \times 10^5$	II $\sigma_{12}^{II} \times 10^5$	III $\sigma_{12}^{III} \times 10^5$
		6.96	1.214	83	1.214	0.739	1.202
		3.94	1.215	82	1.215	0.693	1.192
		2.31	1.399	71	1.399	0.45	1.345
		1.0	1.541	61	1.541	0.235	1.411

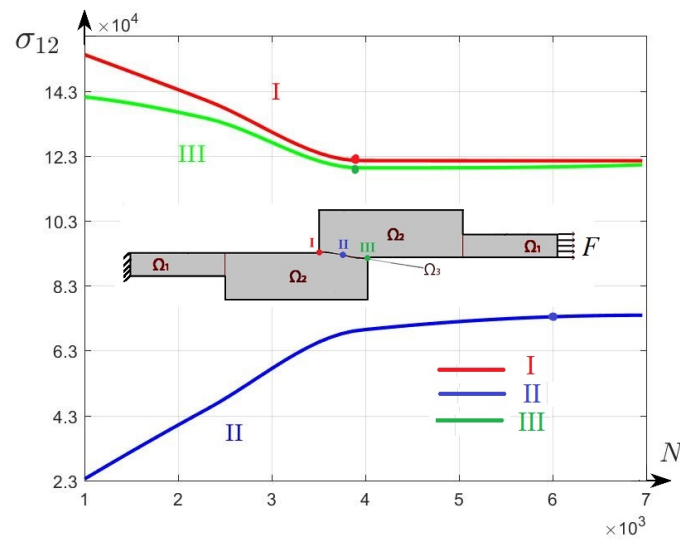


Figure 6. Dependence of shear stresses σ_{12} at points I, II, III on the number FE problem 1. ■ optimal design, ■ Classic type of connection with bevel, ■ Classic type of connection without bevel.

3.2. Case Study 2: Optimization of a Design Consisting of Three Parts Connected with an Overlap

Consider a three-layer elastic structure, the dimensions and boundary conditions for which are given in Figure 6. Region Ω_1 is filled with duralumin with Young’s modulus equal to $E_1 = 73.1 \times 10^6$ Pa, Ω_2 is the area of the topological optimization problem. It requires the optimal microstructure of the distribution of a given amount of duralumin, Ω_3 is the area of evenly distributed silver solder with $E_2 = 2.26 \times 10^6$ Pa. Mechanical load acting on the right $F = 100,000 \frac{H}{m^2}$, the left border is fixed.

Figure 7 displays the three-layer structures commonly used in engineering practice. The construction shown in Figure 7a is similar to Figure 7a and represents an engineering solution for reducing solder stresses. The amount of duralumin and silver solder material used in the constructions depicted in Figure 7a,b is identical to that in the design presented in Figure 7.

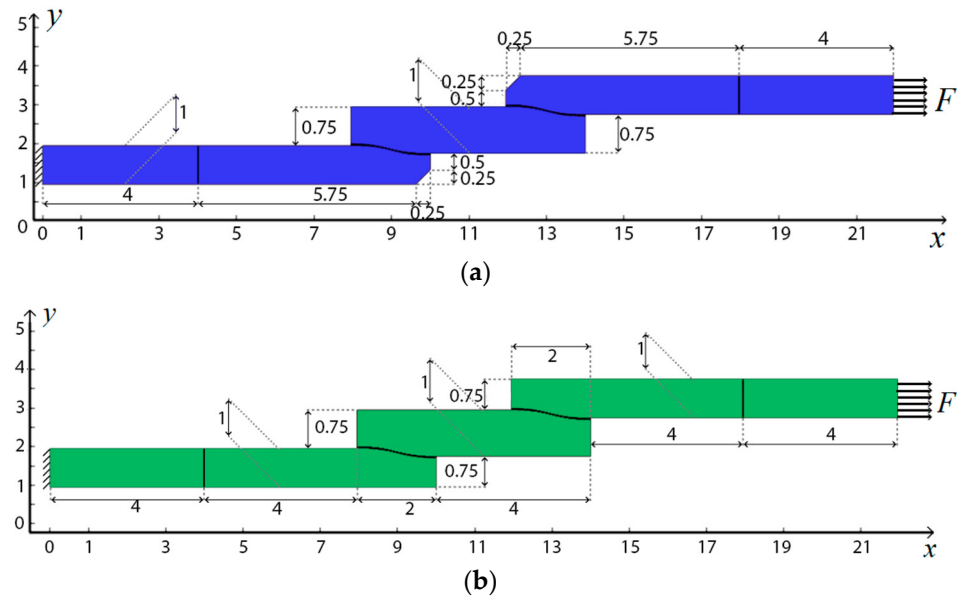


Figure 7. Three-layer constructions with an adhesive layer: (a) ■ Classic type of connection with bevel (B); (b) ■ Classical connection without bevel (C).

Figures 8 and 9 show the distribution of shear stress σ_{12} and Mises stress σ_{Mis} , respectively, in the adhesive layer that connects the middle and upper parts of the structure for cases A, B, C, and D. Qualitatively similar results were obtained for the adhesive layer that connects the lower and middle structures. The graphs depict the stress distribution along the lines that pass through the center of the adhesive layer.

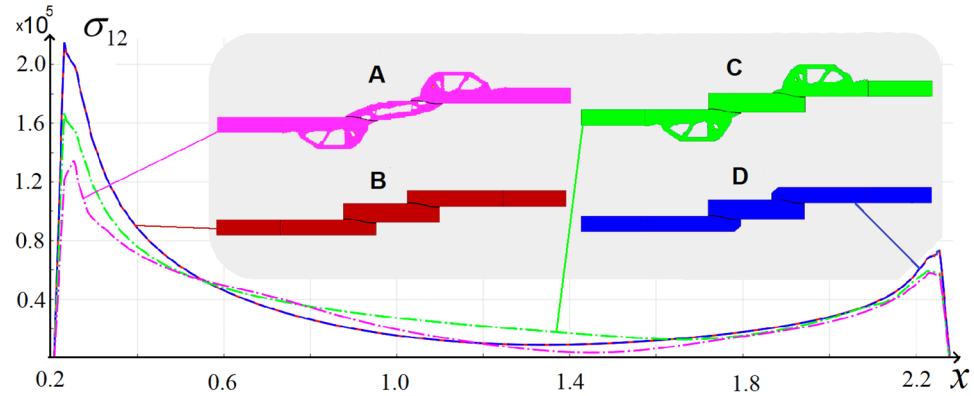


Figure 8. Shear stress (Pa) along the central axis of the solder region. (A) ■ optimal design I, (B) ■ Classic type of connection without bevel, (C) ■ optimal design II, (D) ■ Classic type of connection with bevel.

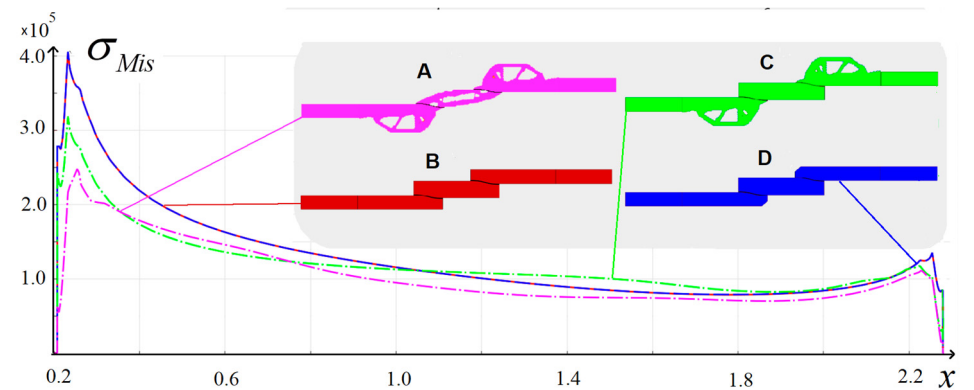


Figure 9. Von Mises stress (Pa) along the central axis of the solder region. (A) ■ optimal design I, (B) ■ Classic type of connection without bevel, (C) ■ optimal design II, (D) ■ Classic type of connection with bevel.

The peak stresses σ_{12} and σ_{Mis} , at the ends of the adhesive for the two types of optimal design (A) and (C) are significantly lower than those of the original design (B) and the beveled design (D) (Figures 8 and 9). It is worth noting that the shear stresses for the optimal design (A) are lower than for all other designs along the entire length of the adhesive layer, indicating the best load-bearing capacity of this design compared with the others.

Table 3 shows the numerical results: Maximum values of Mises stresses in the solder layer, maximum values of shear stresses in the solder layer.

Table 3. Values of maximum stress for Case Study 2.

Construction	Maximum Value σ_{Mis} in Solder	Maximum Shear Stresses σ_{12} in Solder
Straight (initial design) (B)	479,365	243,695
Bevel (engineering option to reduce to shear stresses) (D)	479,840	244,341
Topologically optimal design II (C)	325,920	221,236
Topologically optimal design I (A)	247,865	134,625

The results presented in Table 3 indicate that the maximum values of Mises stresses and shear stresses in the adhesive layer are significantly reduced for the topologically optimal designs (A) and (C) compared with the original design and the beveled design. For the topologically optimal design (C), the maximum values of Mises stresses are reduced by approximately 38%, and the maximum values of shear stresses are reduced by approximately 9%. The topologically optimal design (A) shows even better performance, with a reduction of approximately 49% in the maximum values of Mises stresses and approximately 45% in the maximum values of shear stresses, indicating its superior load-bearing capacity. Regarding problem 1 (Table 1), it should be noted that the engineering option (Table 2, Option D) of reducing shear stresses not only fails to improve the carrying capacity of the original structure but even worsens it (Table 3, Option B). Therefore, the proposed method of minimizing peak Mises and shear stresses (Table 3, Options A and C) is universal and can automatically minimize stresses without the need for manual enumeration of variants. This approach improves the bearing capacity of multilayer composite structures.

In the study, similarly to problem 1, the influence of the number of FEs on the results of solving the optimization problem was investigated in order to justify the validity of the obtained results. The results are given in Table 4 and Figure 10. For maximum shear stress σ_{12} , the difference between result values with the number of FEs 5.18×10^3 and 11.2×10^3 is 0.2%, which confirms the reliability of optimization results. The results shown in Figure 10 show that the stress convergence at the midpoints of the solder solution occurs with number FEs equal to 4.8×10^3 . The stress σ_{12} at the extreme points I and VI is also stabilized with a number of FEs equal to 5.8×10^3 , and at the points (II, IV) the solution is stabilized with a number of FEs equal to 3.8×10^3 . Thus, as in Problem 1, the shear stresses at the solder endpoints (I, III, IV, and VI), both top and bottom, converge faster than for the central points (II, V). The difference from problem 1 is in the other character of stress “equalization”—this process proceeds in pairs. Stresses at the extreme points (I–IV), (III–IV), and at the central points (II–V) are equalized.

Table 4. Dependence $\max\sigma_{12}$ from number of iterations n and σ_{12}^k from number N for FE. ■ left border of adhesive, ■ center point of adhesive, ■ right border of adhesive.

Visualisation of the FE Approximation of an Overlap Joint between Two Beams		Number of Elements $N \times 10^3$	Maximum Stress $\max\sigma_{12} \times 10^5$	Number of Iterations n	$\sigma_{12}^I \times 10^5$	$\sigma_{12}^{II} \times 10^5$	$\sigma_{12}^{III} \times 10^5$	$\sigma_{12}^{IV} \times 10^5$	$\sigma_{12}^V \times 10^5$	$\sigma_{12}^{VI} \times 10^5$
		11.20	1.341	171	1.341	0.211	0.644	0.638	0.198	1.32
		5.18	1.346	164	1.346	0.205	0.655	0.645	0.193	1.331
		2.31	1.995	146	1.852	0.157	0.595	0.637	0.078	1.995
		1.94	2.345	145	2.345	0.038	0.489	0.317	0.071	2.116

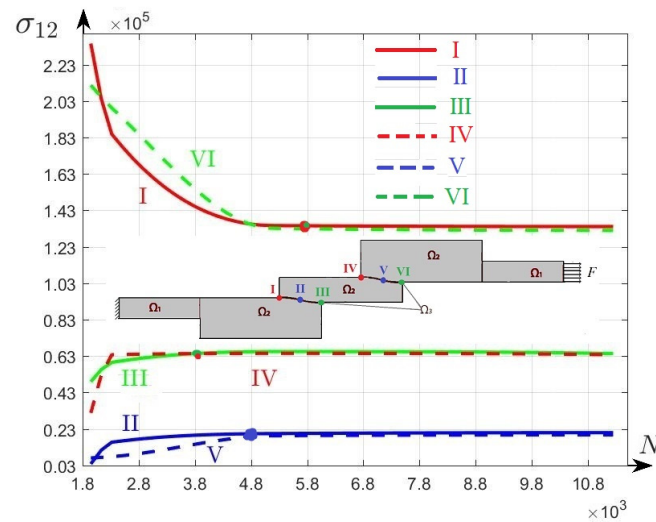


Figure 10. Dependence of shear stresses σ_{12} at points I, II, III of the number of FEs of problem 2. ■ left border of adhesive, ■ center point of adhesive, ■ right border of adhesive.

4. Conclusions

A new algorithm (RAMP and FEM method) for topological optimization in order to reduce peak Mises stresses is developed and used to optimize structures with adhesive layers under longitudinal mechanical loads.

It has been revealed that the algorithm of stress minimization in the adhesive layer, which is based on topological optimization methods, can be used for various geometries of fastened structures and the geometry of the adhesive layer. The universality of the suggested approach will allow its application in a wide area of new engineering soldered structure creation. This approach will allow engineering practice to significantly increase the reliability of developed structures.

The proposed algorithm is shown to be effective in reducing peak Mises stresses in the adhesive layer of multilayer composite joints. The results indicate a reduction of up to 50% in peak stresses compared with the initial design.

The reliability of the obtained optimization results, depending on the number of elements, was investigated. The results shown in Tables 2 and 4 and Figures 6 and 10 are based on the Runge principle a the doubling of the number of elements. The difference in maximum shear stress of the two last finite element partitions for the first problem is 0.06%, while for the second problem it is 0.2%. An increase in the number of finite elements leads to the equalization of joint stresses in the first problem, whereas in the second problem, equalization occurs in pairs.

The use of RAMP interpolation in the optimization phase helps to eliminate the checkerboard effect and improve the quality of the optimal design. The proposed approach can be further extended to include additional design constraints, such as weight or manufacturing constraints, in order to provide more practical designs for engineering applications.

Author Contributions: Conceptualization, A.V.K.; methodology, T.V.Y. and A.V.K.; software, P.V.D.; validation, A.V.K. and V.A.C.; formal analysis, A.V.K. and T.V.Y.; investigation, P.V.D.; writing—original draft preparation, T.V.Y. and A.V.K.; writing—review and editing, A.V.K., visualization, V.A.C.; supervision, A.V.K.; project administration, A.V.K.; funding acquisition, T.V.Y. All authors have read and agreed to the published version of the manuscript.

Funding: This research was supported by the Russian Science Foundation (RSF), Project No. 22-71-10083 (https://rscf.ru/prjcard_int?22-71-10083).

Institutional Review Board Statement: Not applicable.

Informed Consent Statement: Not applicable.

Data Availability Statement: No data was used for the research described in the article.

Conflicts of Interest: The authors declare no conflict of interest.

References

1. Kumar, V.K.; Rao, M.V. Some studies and analysis of adhesive bonded joints: A review. *J. Chin. Adv. Mater. Soc.* **2017**, *5*, 241–253. [CrossRef]
2. Patel, P.; Varikoti, P.; Lama, K. Applications of Composite Material in Aerospace Industry. 2015. Available online: <https://dokumen.tips/engineering/application-of-composite-materials-in-aerospace-industry-1.html?page=1> (accessed on 13 March 2023).
3. He, X. A review of finite element analysis of adhesively bonded joints. *Int. J. Adhes. Adhes.* **2011**, *31*, 248–264. [CrossRef]
4. Banea, M.D.; da Silva, L.F.M. Adhesively bonded joints in composite materials: An overview. *Proc. Inst. Mech. Eng. Part L J. Mater. Des. Appl.* **2009**, *223*, 1–18. [CrossRef]
5. Kahraman, R.; Sunar, M.; Yilbas, B. Influence of adhesive thickness and filler content on the mechanical performance of aluminum single lap-joints bonded with aluminum powder filled epoxy adhesive. *J. Mater. Process. Technol.* **2008**, *205*, 183–189. [CrossRef]
6. Grant, L.D.R.; Adams, R.D.; da Silva, L.F.M. Experimental and numerical analysis of single-lap joints for the automotive industry. *Int. J. Adhes. Adhes.* **2009**, *29*, 405–413. [CrossRef]
7. Vinay, M.N. Optimization of adhesive bonding parameters of aluminium 6082 joints. *AIP Conf. Proc.* **2021**, *2317*, 020042. [CrossRef]
8. Yaman, M.; Şansveren, M.F. Numerical and experimental vibration analysis of different types of adhesively bonded joints. *Structures* **2021**, *34*, 368–380. [CrossRef]
9. Kemiklioglu, U.; Baba, O.B. Vibration effects on tensile properties of adhesively bonded single lap joints in composite materials. *Polym. Compos.* **2019**, *40*, 1258–1267. [CrossRef]
10. Yaman, M.; Şansveren, M.F.; Maraş, S. Vibration characteristics analysis of adhesively bonded different joints. *Turk. J. Electromech. Energy* **2020**, *5*, 21–28.
11. Almitani, K.H.; Othman, R. Analytical solution of the harmonic response of viscoelastic adhesively bonded single-lap and double-lap joints. *Int. J. Adhes. Adhes.* **2016**, *71*, 55–65. [CrossRef]
12. Machado, D.M.S.R.B.; Campilho, R.D.S.G.; Cardoso, M.G. Impact modelling of single-lap bonded joints by cohesive zone models. *Procedia Manuf.* **2019**, *41*, 34–41. [CrossRef]
13. Dragoni, E.; Brinson, H.F. Modeling and optimization of the sandwich beam specimen in three-point bending for adhesive bond characterization. *Int. J. Adhes. Adhes.* **2016**, *68*, 380–388. [CrossRef]
14. Fedorov, A.Y.; Matveenkov, V.P. Designing of interlayers between materials with minimum stress level at the interface. *Int. J. Adhes. Adhes.* **2021**, *111*, 102963. [CrossRef]
15. Valente, J.P.A.; Campilho, R.D.S.G.; Marques, E.A.S.; Machado, J.J.M.; da Silva, L.F.M. Geometrical optimization of adhesive joints under tensile impact loads using cohesive zone modeling. *Int. J. Adhes. Adhes.* **2020**, *97*, 102492. [CrossRef]
16. Valente, J.P.A.; Campilho, R.D.S.G.; Marques, E.A.S.; Machado, J.J.M.; da Silva, L.F.M. Adhesive joint analysis under tensile impact loads by cohesive zone modelling. *Compos. Struct.* **2019**, *222*, 110894. [CrossRef]
17. Ejaza, H.; Mubashara, A.; Ashcroft, I.A.; Uddina, E.; Khanc, M. Topology optimisation of adhesive joints using non-parametric methods. *Int. J. Adhes. Adhes.* **2018**, *81*, 1–10. [CrossRef]
18. de Vicente, M. Numerical optimization of hybrid panel joints by mixed adhesive/welded method on shipbuilding. In Proceedings of the ASME 2018 37th International Conference on Ocean, Offshore and Arctic Engineering OMAE2018, Madrid, Spain, 17–22 June 2018. [CrossRef]
19. de Vicente, M.; Silva-Campillo, A.; Herreros, M.Á.; Suárez-Bermejo, J.C. Design of a structurally welded/adhesively bonded joint between a fiber metal laminate and a steel plate for marine applications. *J. Mar. Sci. Technol.* **2022**, *27*, 1002–1014. [CrossRef]
20. Kim, C.; Seong, H.K.; Kim, I.Y.; Yoo, J. Single variable-based multi-material structural optimization considering interface behavior. *Comput. Methods Appl. Mech. Engng.* **2020**, *367*, 113114. [CrossRef]
21. Arhore, E.G.; Yasae, M.; Dayyani, I. Comparison of GA and topology optimization of adherend for adhesively bonded metal composite joints. *Int. J. Solids Struct.* **2021**, *226–227*, 111078. [CrossRef]
22. Mallick, P.K. Optimization of Structural Adhesive Joints. In *Structural Adhesive Joints: Design, Analysis and Testing*; Mittal, K.L., Panigrahi, S.K., Eds.; Wiley: Hoboken, NJ, USA, 2020. [CrossRef]
23. Hamdia, K.M.; Ghasemi, H.; Zhuang, X.; Rabczuk, T. Multilevel Monte Carlo method for topology optimization of flexoelectric composites with uncertain material properties. *Eng. Anal. Bound. Elem.* **2022**, *134*, 412–418. [CrossRef]
24. Awrejcewicz, J.; Pavlov, S.P.; Krysko, A.V.; Zhigalov, M.V.; Bodyagina, K.S.; Krysko, V.A. Decreasing Shear Stresses of the Solder Joints for Mechanical and Thermal Loads by Topological Optimization. *Materials* **2020**, *13*, 1862. [CrossRef] [PubMed]
25. Krysko, A.V.; Awrejcewicz, J.; Dunchenkin, P.V.; Zhigalov, M.V.; Krysko, V.A. Topological Optimization of Multilayer Structural Elements of MEMS/NEMS Resonators with an Adhesive Layer Subjected to Mechanical Loads. In *Recent Approaches in the Theory of Plates and Plate-like Structures. Advanced Structured Materials*; Altenbach, H., Bauer, S., Eremeyev, V.A., Mikhasev, G.I., Morozov, N.F., Eds.; Springer: Cham, Switzerland, 2022; Volume 151. [CrossRef]

26. Brackett, D.; Panesar, A.; Ashcroft, I.; Wildman, R.; Hague, R. An optimisation based design framework for multifunctional 3D printing. In *24th Annual International Solid Freeform Fabrication Symposium: An Additive Manufacturing Conference, Proceedings, 12–14 August 2013*; Solid Freeform Fabrication Proceedings; University of Texas: Austin, TX, USA, 2013; ISSN 1053-2153.
27. Tang, Y.; Zhao, Y.F. A survey of the design methods for additive manufacturing to improve functional performance. *Rapid Prototyp. J.* **2016**, *22*, 569–590. [[CrossRef](#)]
28. Panesar, A.; Brackett, D.; Ashcroft, I.; Wildman, R.; Hague, R. Design Framework for Multifunctional Additive Manufacturing: Placement and Routing of Three-Dimensional Printed Circuit Volumes. *ASME J. Mech. Des.* **2015**, *137*, 111414. [[CrossRef](#)]
29. Ozguc, S.; Pan, L.; Weibel, J.A. Topology optimization of microchannel heat sinks using a homogenization approach. *Int. J. Heat Mass Transf.* **2021**, *169*, 120896. [[CrossRef](#)]
30. Gu, X.; He, S.; Dong, Y.; Song, T. An improved ordered SIMP approach for multiscale concurrent topology optimization with multiple microstructures. *Compos. Struct.* **2022**, *287*, 115363. [[CrossRef](#)]
31. Kotarski, D.; Piljek, P.; Pranjić, M.; Grlj, C.G.; Kasać, J. A Modular Multirotor Unmanned Aerial Vehicle Design Approach for Development of an Engineering Education Platform. *Sensors* **2021**, *21*, 2737. [[CrossRef](#)]
32. Chen, Z.; Rahimi Nohooji, H.; Chew, C. Development of Topology Optimized Bending-Twisting Soft Finger. *J. Mech. Robot.* **2021**, *14*, 051003. [[CrossRef](#)]
33. Tyflopoulos, E.; Steinert, M. A Comparative Study of the Application of Different Commercial Software for Topology Optimization. *Appl. Sci.* **2022**, *12*, 611. [[CrossRef](#)]
34. Bendsoe, M.P.; Sigmund, O. Topology Optimization. In *Theory, Methods and Applications*; Springer: Berlin/Heidelberg, Germany, 2004. [[CrossRef](#)]
35. Awrejcewicz, J.; Pavlov, S.P.; Bodyagina, K.S.; Zhigalov, M.V.; Krysko, V.A. Design of composite structures with extremal elastic properties in the presence of technological constraints. *Compos. Struct.* **2017**, *174*, 19–25. [[CrossRef](#)]
36. Krysko, A.V.; Awrejcewicz, J.; Pavlov, S.P.; Bodyagina, K.S.; Zhigalov, M.V.; Krysko, V.A. Non-linear dynamics of size-dependent Euler–Bernoulli beams with topologically optimized microstructure and subjected to temperature field. *Int. J. Non-Linear Mech.* **2018**, *104*, 75–86. [[CrossRef](#)]
37. Krysko, A.; Awrejcewicz, J.; Bodyagina, K.; Makseev, A.; Zhigalov, M.; Krysko, V. Identifying inclusions in a non-uniform thermally conductive plate under external flows and internal heat sources using topological optimization. *Math. Mech. Solids* **2022**, *27*, 1649–1671. [[CrossRef](#)]
38. Krysko, A.V.; Makseev, A.; Smirnov, A.; Zhigalov, M.V.; Krysko, V.A. A New Approach to Identifying an Arbitrary Number of Inclusions, Their Geometry and Location in the Structure Using Topological Optimization. *Appl. Sci.* **2023**, *13*, 49. [[CrossRef](#)]

Disclaimer/Publisher’s Note: The statements, opinions and data contained in all publications are solely those of the individual author(s) and contributor(s) and not of MDPI and/or the editor(s). MDPI and/or the editor(s) disclaim responsibility for any injury to people or property resulting from any ideas, methods, instructions or products referred to in the content.